Thai Journal of Mathematics
Volume 22 Number 1 (2024)
Pages 35–63

http://thaijmath.in.cmu.ac.th

ISSN 1686-0209

Annual Meeting in Mathematics 2023

Mathematical Models for Brown Planthopper Infestation of Rice under Habitat Complexity and Monsoon Effects

Nattawut Khansai[1], **Sekson Sirisubtawee**[1,2,*], **Sanoe Koonprasert**[1,2], **Watchareewan Jamboonsri**[3] **and Wisut Kitchainukoon**[4]

[1] *Department of Mathematics, Faculty of Applied Science, King Mongkut's University of Technology North Bangkok, Bangkok 10800, Thailand*
e-mail : nattawut.khansai@gmail.com (N. Khansai); sekson.s@sci.kmutnb.ac.th (S. Sirisubtawee); sanoe.k@sci.kmutnb.ac.th (S. Koonprasert)

[2] *Centre of Excellence in Mathematics, CHE, Si Ayutthaya Road, Bangkok 10400, Thailand*

[3] *Innovative Plant Biotechnology and Precision Agriculture Research Team, National Center for Genetic Engineering and Biotechnology (BIOTEC), National Science and Technology Development Agency (NSTDA), Khlong Nueng, Pathum Thani 12120, Thailand*
e-mail : watchareewan@biotec.or.th (W. Jamboonsri)

[4] *Department of Mathematics, Faculty of Science and Technology, Loei Rajabhat University, Loei 42000, Thailand*
e-mail : wisut.kit@lru.ac.th (W. Kitchainukoon)

Abstract In this research, we study mathematical predator-prey models for brown planthopper (BPH) infestation of rice under the effects of habitat complexity and monsoon for two time scales. Using a fast time scale, we obtain a complete model which is a system of first-order differential equations including logistic growth terms, modified Holling type II functional responses and migration terms due to the monsoon. The positivity and boundedness of the fast time-scale model are proved. Using a slow time scale and the aggregated method, we obtain an aggregated model which is less complicated than the former model in terms of the number of variables and parameters. We investigate the existence of equilibrium points and their local asymptotic stability for this aggregrated model. Hopf bifurcation of the aggregrated model is also shown to occur as the maximum carrying capacity is varied. Numerical simulations are performed to illustrate the theoretical results. Finally, some ecological discussion of methods for reducing the BPH dispersion of the model is given.

MSC: 92-10; 37N25; 92B05

Keywords: brown planthopper; monsoon effect; aggregated method; modified Holling type II functional response; hopf bifurcation

Submission date: 02.06.2023 / Acceptance date: 31.08.2023

*Corresponding author.

Published by The Mathematical Association of Thailand.

1. Introduction

The brown planthopper (BPH), *Nilaparvata lugens* (Stål) is a major pest in rice production. Because of its survival behavior it continually migrates to new vulnerable areas of rice fields. There are two main types of BPH, namely long-winged BPH and short-winged BPH. The long-winged BPH can migrate for both short and long distances while the short-winged BPH can only move for short distances [1]. In the past decade, the migration of BPHs has been discussed several times in the literature [2–4]. Its migration normally occurs under the influence of the monsoon, which blows seasonally for a period of about six months and in a specific direction [2].

Major factors in BPH migration are landscape and complexity of the habitat. Habitat structure includes both biotic and abiotic features such as light, humidity, topography, rainfall, light traps, etc. [5, 6]. This habitat structure also affects the population density of predators of BPH. Some examples indicating the significant role of habitat in predator-prey systems can be found in [7–11].

Rice is both a resident plant and a food plant and the properties of the rice and the rice fields have an impact on the survival of plant pathogens and transmission of rice viruses as well as on the survival of BHP. Since rice is a host of BPH, it is important for BPH survival and affects BPH propagation. The planting of resistant rice varieties in rice fields can therefore reduce the population density of the insect and the damage it can cause. In addition, the distance between the rice plants, the amount and type of pesticides used, weeds, BPH traps, and natural enemies of the BPH can also be used to reduce the attack of BPHs on the rice.

There are now many types of mathematical models that have been developed to study the foraging and survival behavior of organisms in ecosystems in areas such as ecology, biology, and entomology [12–16]. Predator-prey models have been commonly used to study systems in which one species, the prey, is the food of another species, the predator [13, 15–17]. A recent literature review of predator-prey models can be found in [18–20]. In addition, aggregation methods [21, 22] are a compromise between big systems and simple ones exhibiting different time scales associated with the dynamics of variables. The time scales usually consist of a fast time scale at the individual level and a slow one at the population or community level. Methods have been developed for ecological models in order to seek for necessary conditions from which a reduced set of differential equations governing aggregated variables is obtained. Normally, we assume that the migration process taking place for each individual has a shorter time scale compared to the population time scale.

Some of the previous studies of habitat complexity and migration effects are as follows. In 2007, Mchich et al. [23] introduced the Lotka-Volterra model on two patches. In 2011, Bairagi and Jana [24] studied a delayed predator-prey model with a Holling type II functional response. They analyzed the stability of the system and the properties of Hopf bifurcations that can occur in the system. In 2012, Doanh et al. [25] studied a model for two competing species in a two patch environment. They showed that some species use a density-dependent dispersal strategy to prevent their own extinction. Also, they showed the importance of refuges in predator-prey systems. In 2014, Jana and Bairagi [5] developed the Rosenzweig-MacArthur model in order to investigate how habitat complexity affects a predator-prey system. Also, in 2014, Hieu et al. [26] studied a model of fish migration with both small and large clusters. According to their results, fish populations scattered in small and large groups are most effective for small maritime fisheries. In 2021, Zhang et al. [20] proposed a stochastic predator-prey model containing prey aggregation and habitat complexity. Their findings demonstrated the importance of prey aggregation, habitat complexity, and environmental noise in affecting the survival and extinction of the system. In 2022, Nguyen et al. [27] used the aggregated method on a predator-prey model to study the impact of a monsoon on the rice-BPH relationship. They proved the stability of the system and the existence of a Hopf bifurcation. In this paper, we are interested in studying the effects of degree of habitat complexity included in a functional response and of migration of BHP during the monsoon season. These two factors have not been incorporated together in any predator-prey models appearing in previous investigations.

The remainder of this paper is organized as follows. In section 2, we present our complete mathematical model for BPH infestation of rice which includes the effects of habitat complexity and the monsoon. A derivation of the model and a definition of all variables and parameters are given. We then establish the conditions for the positivity and boundedness of the solutions of the model. At the end of this section, we propose an aggregated model which is our main model for analysis of the BPH-rice system. In section 3, we find the equilibrium points of the aggregated model, analyze their stability and determine conditions for Hopf bifurcation. In section 4, we present numerical results for the model for a range of parameter values. Finally, in section 5 we discuss the conclusions of this research.

2. Model Derivation

We begin this section by introducing the Holling type II functional response which can be defined as [24, 28]:

$$\Psi(\xi) = \frac{a\xi}{1 + ah\xi}, \tag{2.1}$$

where the variable ξ denotes the prey population density and the parameters a, h represent the attack rate and the handling time, respectively. However, the above function does not include the degree or strength of habitat complexity. A modified Holling type II functional response which incorporates an effect of habitat complexity through a parameter ν where $0 < \nu < 1$ can be written as [5, 20, 24]:

$$\Psi(\xi) = \frac{a(1-\nu)\xi}{1 + ah(1-\nu)\xi}. \tag{2.2}$$

If $\nu = 0$, then Eq. (2.2) obviously reduces to Eq. (2.1). The modified Holling type II functional response (2.2) is appropriate for the predator-prey interaction with habitat complexity [24]. Figure 1 shows the relationships between the prey density (ξ) and the consumed prey ($\Psi(\xi)$) when the degree of habitat complexity ν is varied with the parameter values of a and h fixed at 0.85 and 0.8, respectively.

Next, we assume that we have two fields with variables and parameters of fields labeled by $i = 1, 2$. For ease of reading, the definitions of all variables and parameters used in our model are given in Table 1.

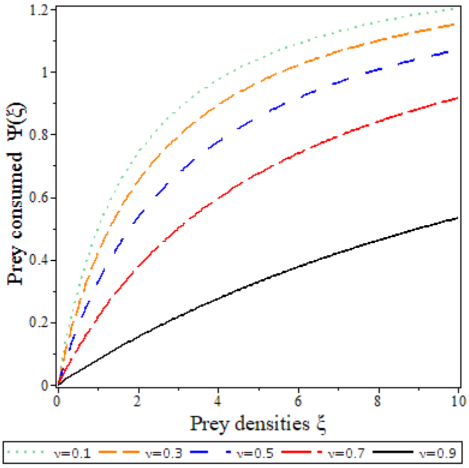

FIGURE 1. Relationships between the prey density ξ and the consumed prey $\Psi(\xi)$ satisfying Eq. (2.2) when ν is varied and $a = 0.85$, $h = 0.8$.

TABLE 1. Meaning of variables and parameters used in our models [20, 27].

Variables/ Parameters	Ecological meaning (unit)
t	Slow time scale (Time)
τ	Fast time scale (Time)
ε	Ratio between slow and fast time scales (dimensionless)
R_i	Population density of rice (Population density)
B_i	Population density of BPH (Population density)
B	Total population density of BPH from fields 1 and 2 (Population density)
r_i	Intrinsic growth rate (Time^{-1})
K	Maximum carrying capacity of rice for each field (Population density)
a_i	Attack rates of BPH (Population density$\times$Time^{-1})
h_i	Handling times of BPH (Time$\times$Population density^{-1})
ν_i	Degree of habitat complexity (dimensionless)
e_i	Conversion coefficient (dimensionless)
d_i	Natural death rate of BPH (Time^{-1})
$\bar{m}$	Per capita dispersal rate in the opposite direction to the wind (Time^{-1})
m_0	Per capita density-independent dispersal rate from field 1 (Time^{-1})
m_1	Strength of density-dependence in dispersal from field 1 (Time^{-1})

Since a logistic term can describe an interaction of biotic potential with environmental resources, we consider that the growth rate of rice can be expressed in terms of the logistic model with the intrinsic growth rate r_i for field i and maximum carrying capacity K for each field. For simplicity, we assume that BPH is the rice's only enemy and that its consumption rate for each field follows the modified Holling type II functional response with the attack rate a_i, the handling time h_i and the degree of habitat complexity ν. For example, $\nu = 0.1$ means that the complexity of the area results in a 10% reduction in hunting efficiency. Furthermore, we assume that the BPH migration caused by the monsoon has only one main direction from field 1 to field 2. Under the impact of the monsoon and the dependence on the population density in the starting field 1, the effect of the monsoon is modeled by a linear function of the BPH density in field 1 with the density-independent dispersal rate m_0 and the density-dependent dispersal rate m_1. In addition, the dispersal rate in the opposite direction is denoted by $\bar{m}$.

We begin by constructing a complete model for the BPH-rice system with a fast time scale τ for the fast dispersal of the BPH by the monsoon. Then, we will use the aggregation method [25, 26] to reduce the dimension of the complete model in order to obtain a less sophisticated model with a slow time scale t called the aggregrated model. The total density of BPH in both fields for the aggregrated model is not affected by the rapid dispersal but depends upon the competition process between the natural growth of the rice and the predation by the BPH. The parameter $\varepsilon = \frac{t}{\tau}$ represents the ratio between the slow and fast time scales and is multiplied into terms of the slow process. Based on the above assumptions, the complete model for the relationship between rice and BPH can be written as:

$$\begin{aligned}
\frac{dR_1}{d\tau} &= F_1(R_1, R_2, B_1, B_2) = \varepsilon \left[r_1 R_1 \left(1 - \frac{R_1}{K}\right) - \frac{a_1(1-\nu_1)R_1B_1}{1 + a_1h_1\,(1-\nu_1)\,R_1} \right], \\
\frac{dR_2}{d\tau} &= F_2(R_1, R_2, B_1, B_2) = \varepsilon \left[r_2 R_2 \left(1 - \frac{R_2}{K}\right) - \frac{a_2(1-\nu_2)R_2B_2}{1 + a_2h_2\,(1-\nu_2)\,R_2} \right], \\
\frac{dB_1}{d\tau} &= F_3(R_1, R_2, B_1, B_2) = \varepsilon \left[\frac{e_1a_1(1-\nu_1)R_1B_1}{1 + a_1h_1\,(1-\nu_1)\,R_1} - d_1B_1 \right] + \left[\bar{m}B_2 - (m_0 + m_1B_1)\,B_1\right], \\
\frac{dB_2}{d\tau} &= F_4(R_1, R_2, B_1, B_2) = \varepsilon \left[\frac{e_2a_2(1-\nu_2)R_2B_2}{1 + a_2h_2\,(1-\nu_2)\,R_2} - d_2B_2 \right] + \left[(m_0 + m_1B_1)\,B_1 - \bar{m}B_2\right],
\end{aligned} \tag{2.3}$$

along with the initial conditions $R_i(0) \geq 0$, $B_i(0) \geq 0$, $i = 1, 2$. Figure 2 shows a diagram of the complete model (2.3).

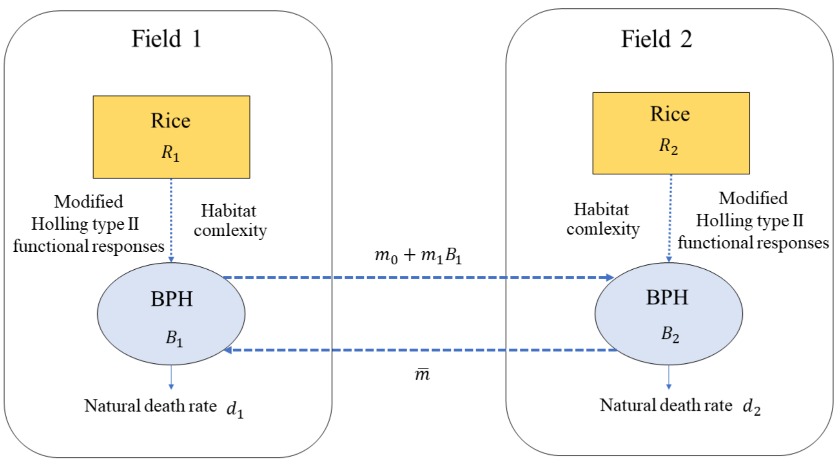

FIGURE 2. Diagram of BPH and rice dynamical system with monsoon and habitat complexity factors. In each field, rice and BPH are the two variables in the complete model. Growth, predation and dispersion are the three main processes appearing in the model.

2.1. Positivity and Boundedness

In this section, we investigate the positivity and boundedness of the complete model (2.3). Denoting $\mathbb{R}^4_+$ as the state space consisting of four components whose values are greater than or equal to zero, we have the following theorem.

Theorem 2.1. *All of the solutions of system* (2.3) *are positive and bounded if the system starts in* $\mathbb{R}^4_+$.

Proof. Let

$$\Omega^+ = \{x = (R_1, R_2, B_1, B_2) \in \mathbb{R}^4_+ \,:\, R_i, B_i \geq 0,\, i = 1, 2\} \tag{2.4}$$

be the non-negative cone which $(R_1(0), R_2(0), B_1(0), B_2(0)) \in \Omega^+$. Assume that $R_1 \geq 0, R_2 \geq 0, B_1 \geq 0$ and $B_2 \geq 0$, we then have

$$\begin{aligned} &F_1(0, R_2, B_1, B_2) = 0, \\ &F_2(R_1, 0, B_1, B_2) = 0, \\ &F_3(R_1, R_2, 0, B_2) = \bar{m}B_2 \geq 0, \\ &F_4(R_1, R_2, B_1, 0) = (m_0 + m_1 B_1)B_1 \geq 0. \end{aligned} \tag{2.5}$$

Therefore, by using a theorem in [29], we obtain $(R_1(t), R_2(t), B_1(t), B_2(t)) \in \Omega_+$ with $t = \varepsilon\tau \in \mathbb{R}^+$. Hence, the solutions are still contained in $\mathbb{R}^4_+$ and the positivity of the solutions is then derived.

Considering the first and second equations of (2.3), we have

$$\frac{dR_1}{d\tau} \leq \varepsilon \left[r_1 R_1 \left(1 - \frac{R_1}{K} \right) \right] \Rightarrow \limsup_{t \to \infty} R_1(t) = K, \tag{2.6}$$

and

$$\frac{dR_2}{d\tau} \leq \varepsilon \left[r_2 R_2 \left(1 - \frac{R_2}{K} \right) \right] \Rightarrow \limsup_{t \to \infty} R_2(t) = K, \tag{2.7}$$

with $t = \varepsilon\tau$.

Let $W(t) = R_1(t) + R_2(t) + B_1(t) + B_2(t)$ and $\sigma \in \mathbb{R}$ will be chosen later. Then, by using (2.3), we have

$$\begin{aligned} \frac{dW}{dt} + \sigma W = r_1 R_1 \left(1 - \frac{R_1}{K}\right) &- \frac{(1-e_1)(1-\nu_1)a_1 R_1 B_1}{1 + a_1 h_1 (1-\nu_1) R_1} - d_1 B_1 \\ + r_2 R_2 \left(1 - \frac{R_2}{K}\right) &- \frac{(1-e_2)(1-\nu_2)a_2 R_2 B_2}{1 + a_2 h_2 (1-\nu_2) R_2} - d_2 B_2 \\ + \sigma R_1 + \sigma R_2 + \sigma B_1 + \sigma B_2&. \end{aligned} \tag{2.8}$$

Since $0 < e_1,\, e_2,\, \nu_1,\, \nu_2 < 1$, we have

$$\begin{aligned} \frac{dW}{dt} + \sigma W \leq r_1 R_1 \left(1 - \frac{R_1}{K}\right) + r_2 R_2 \left(1 - \frac{R_2}{K}\right)& \\ + \sigma R_1 + \sigma R_2 - (d_1 - \sigma)B_1 - (d_2 - \sigma)B_2&. \end{aligned} \tag{2.9}$$

Choosing $\sigma = \min\{d_1, d_2\}$ and using (2.6) and (2.7), we get

$$\begin{aligned}\frac{dW}{dt} + \sigma W &\leq \left[r_1 R_1 \left(1 - \frac{R_1}{K}\right) + \sigma R_1\right] + \left[r_2 R_2 \left(1 - \frac{R_2}{K}\right) + \sigma R_2\right] \\ &\leq (r_1 + \sigma) R_1 + (r_2 + \sigma) R_2 \\ &\leq [(r_1 + \sigma) + (r_2 + \sigma)] K \equiv M. \end{aligned} \tag{2.10}$$

From (2.10), we obtain

$$0 \leq W(t) \leq \frac{M}{\sigma} + W(0) \exp(-\sigma t) \tag{2.11}$$

and consequently

$$0 \leq \lim_{t \to \infty} W(t) \leq \frac{M}{\sigma}. \tag{2.12}$$

Therefore, the boundedness of the solutions of model (2.3) is verified. ■

Moreover, it is obvious that the right-hand side functions $F_i(R_1, R_2, B_1, B_2)$, $i = 1, 2, 3, 4$ have continuous first partial derivatives with respect to all variables which are positive and bounded. Consequently, the uniqueness of a solution of system (2.3) is established when any given initial conditions in $\mathbb{R}^4_+$ are provided.

2.2. Derivation of the Aggregated Model

In this section, we use the aggregated approach with the relation $t = \varepsilon\tau$ to simplify the complete model (2.3). Defining $B = B_1 + B_2$ as the total population of BPH, then system (2.3) becomes

$$\begin{aligned}\frac{dR_1}{d\tau} &= \varepsilon \left[r_1 R_1 \left(1 - \frac{R_1}{K}\right) - \frac{a_1(1-\nu_1) R_1 B_1}{1 + a_1 h_1 (1-\nu_1) R_1}\right], \\ \frac{dR_2}{d\tau} &= \varepsilon \left[r_2 R_2 \left(1 - \frac{R_2}{K}\right) - \frac{a_2(1-\nu_2) R_2 (B - B_1)}{1 + a_2 h_2 (1-\nu_2) R_2}\right], \\ \frac{dB_1}{d\tau} &= \varepsilon \left[\frac{e_1 a_1(1-\nu_1) R_1 B_1}{1 + a_1 h_1 (1-\nu_1) R_1} - d_1 B_1\right] + [\bar{m}(B - B_1) - (m_0 + m_1 B_1) B_1], \\ \frac{dB}{d\tau} &= \varepsilon \left[\frac{e_2 a_2 (1-\nu_2) R_2 (B - B_1)}{1 + a_2 h_2 (1-\nu_2) R_2} - d_2 (B - B_1) + \frac{e_1 a_1 R_1 B_1}{1 + a_1 h_1 (1-\nu_1) R_1} - d_1 B_1\right]. \end{aligned} \tag{2.13}$$

Substituting $\varepsilon = 0$ into (2.13) and finding a fast equilibrium point of the complete model (2.13), we have that

$$\bar{m}(B - B_1) - (m_0 + m_1 B_1) B_1 = 0, \tag{2.14}$$

or

$$B_1^2 + \frac{(\bar{m} + m_0)}{m_1} B_1 - \frac{\bar{m}}{m_1} B = 0. \tag{2.15}$$

From (2.15), we obtain $B_1 (> 0)$ in the terms of B as follows:

$$B_1 = -\mu_1 + \sqrt{\mu_1^2 + \mu_2 B}, \tag{2.16}$$

where

$$\mu_1 = \frac{m_0 + \bar{m}}{2m_1} \quad \text{and} \quad \mu_2 = \frac{\bar{m}}{m_1}. \tag{2.17}$$

Using the relations $B_1 = B - B_2$, $\frac{dB_1}{dt} = \frac{dB}{dt} - \frac{dB_2}{dt}$, (2.16), the fourth equation of (2.3) and the condition (2.14), system (2.13) can be reduced to system (2.18) from which the variable B_1 disappears. Hence, the aggregated model, which only remains on the slow-time scale t, is obtained as follows:

$$\begin{aligned}
\frac{dR_1}{dt} =& f_1(R_1,R_2,B) = r_1R_1\left(1-\frac{R_1}{K}\right) - \frac{a_1(1-\nu_1)R_1\left(-\mu_1+\sqrt{\mu_1^2+\mu_2 B}\right)}{1+a_1h_1\left(1-\nu_1\right)R_1},\\
\frac{dR_2}{dt} =& f_2(R_1,R_2,B) = r_2R_2\left(1-\frac{R_2}{K}\right) - \frac{a_2(1-\nu_2)R_2\left(B+\mu_1-\sqrt{\mu_1^2+\mu_2 B}\right)}{1+a_2h_2\left(1-\nu_2\right)R_2},\\
\frac{dB}{dt} =& f_3(R_1,R_2,B) = \frac{e_2a_2(1-\nu_2)R_2\left(B+\mu_1-\sqrt{\mu_1^2+\mu_2 B}\right)}{1+a_2h_2\left(1-\nu_2\right)R_2} - d_2\left(B+\mu_1-\sqrt{\mu_1^2+\mu_2 B}\right)\\
&+\frac{e_1a_1(1-\nu_1)R_1\left(-\mu_1+\sqrt{\mu_1^2+\mu_2 B}\right)}{1+a_1h_1\left(1-\nu_1\right)R_1} - d_1\left(-\mu_1+\sqrt{\mu_1^2+\mu_2 B}\right).
\end{aligned} \tag{2.18}$$

3. Analysis of the Aggregated Model

In this section, we investigate the existence of equilibrium points of the aggregated model (2.18). In addition, the local stability of all of the equilibrium points is established. Finally, the Hopf bifurcation of the model is derived.

3.1. Existence of Equilibrium Points

The aggregated model (2.18) has the following seven equilibrium points:

(i) The vanishing equilibrium $E_0(0,0,0)$ always occurs. This corresponds to the case that populations of rice and BPH are absent on both fields.

(ii) The axial equilibrium point $E_1(K,0,0)$ always exists.

(iii) The axial equilibrium point $E_2(0,K,0)$ always exists.

(iv) The ideal equilibrium point (i.e., the BPH-free equilibrium point) $E_3(K,K,0)$ always occurs. This means the BPH becomes extinct and rice grows to the maximum capacity on both fields.

(v) The equilibrium point $E_4(0,\hat{R}_2,\hat{B})$ is associated with the case that the BPH have depleted all rice on field 1, but rice on field 2 still remains. The expressions of $\hat{R}_2$ and $\hat{B}$ can be implicitly written as

$$\hat{B} = \frac{\left(b_0\hat{R}_2+b_1\right)\left(b_2\hat{R}_2+d_1-d_2\right)}{\left(b_3\hat{R}_2+d_2\right)^2}, \tag{3.1}$$

where $\hat{R}_2 > \frac{d_2-d_1}{b_2} \geq 0$ and $\hat{R}_2$ must satisfy the following equation

$$\begin{aligned}
r_2\hat{R}_2\left(1-\frac{\hat{R}_2}{K}\right) - \frac{a_2(1-\nu_2)\hat{R}_2}{1+a_2h_2\left(1-\nu_2\right)\hat{R}_2}\Bigg\{&\left(\frac{\left(b_0\hat{R}_2+b_1\right)\left(b_2\hat{R}_2+d_1-d_2\right)}{\left(b_3\hat{R}_2+d_2\right)^2}\right)\\
&+\mu_1-\sqrt{\mu_1^2+\mu_2\left(\frac{\left(b_0\hat{R}_2+b_1\right)\left(b_2\hat{R}_2+d_1-d_2\right)}{\left(b_3\hat{R}_2+d_2\right)^2}\right)}\Bigg\} = 0,
\end{aligned} \tag{3.2}$$

where

$$\begin{aligned} b_0 &= a_2\left(1-\nu_2\right)\left(\left(\left(d_1-d_2\right)h_2+e_2\right)\mu_2+2\,\mu_1\left(d_2h_2-e_2\right)\right),\\ b_1 &= \left(d_1-d_2\right)\mu_2+2\,d_2\mu_1,\\ b_2 &= a_2\left(1-\nu_2\right)\left(\left(d_1-d_2\right)h_2+e_2\right),\\ b_3 &= a_2\left(1-\nu_2\right)\left(d_2h_2-e_2\right). \end{aligned} \tag{3.3}$$

(vi) The equilibrium point $E_5(\tilde{R}_1, 0, \tilde{B})$ corresponds to the extinction of rice on field 2 due to the BPH migration but some rice population on field 1 still exists. The expressions of $\tilde{R}_1$ and $\tilde{B}$ can be implicitly obtained from

$$\tilde{B} = \frac{\left(c_0\,\tilde{R}_1+c_1\right)\left(c_2\,\tilde{R}_1+d_1-d_2\right)}{d_2^2\left(c_3\,\tilde{R}_1+1\right)^2}, \tag{3.4}$$

where $\tilde{R}_1 > \frac{d_2-d_1}{c_2} \geq 0$ and $\tilde{R}_1$ must satisfy the following equation:

$$\begin{aligned} r_1\tilde{R}_1\left(1-\frac{\tilde{R}_1}{K}\right) &- \frac{a_1(1-\nu_1)\tilde{R}_1}{1+a_1h_1\left(1-\nu_1\right)\tilde{R}_1}\\ &\times\left\{-\mu_1+\sqrt{\mu_1^2+\mu_2\left(\frac{\left(c_0\,\tilde{R}_1+c_1\right)\left(c_2\,\tilde{R}_1-d_1+d_2\right)}{{d_2}^2\left(c_3\,\tilde{R}_1+1\right)^2}\right)}\right\}=0, \end{aligned} \tag{3.5}$$

where

$$\begin{aligned} c_0 &= a_1\left(1-\nu_1\right)\left(\left(\left(d_1-d_2\right)h_1-e_1\right)\mu_2+2\,d_2h_1\mu_1\right),\\ c_1 &= \left(d_1-d_2\right)\mu_2+2\,d_2\mu_1,\\ c_2 &= a_1\left(1-\nu_1\right)\left(\left(d_1-d_2\right)h_1-e_1\right),\\ c_3 &= a_1\left(1-\nu_1\right)h_1. \end{aligned} \tag{3.6}$$

(vii) The co-existence equilibrium point $E^*(R_1^*, R_2^*, B^*)$ corresponds to the case that rice and BPH remain on both fields where the positive values of R_1^* and R_2^* are implicitly defined in terms of B^* as

$$R_1^* = p_1+\sqrt{p_2-p_3\sqrt{\mu_1^2+\mu_2B^*}}, \quad R_2^* = q_1+\sqrt{q_2+q_3\sqrt{\mu_1^2+\mu_2B^*}-q_3B^*}, \tag{3.7}$$

where

$$\begin{aligned} p_1 &= \frac{a_1\left(1-\nu_1\right)h_1K-1}{2a_1\left(1-\nu_1\right)h_1},\ p_2=\frac{K^2}{4}+\frac{k_1\mu_1}{h_1r_1}+\frac{K}{2a_1\left(1-\nu_1\right)h_1}+\frac{1}{4\left(a_1\left(1-\nu_1\right)h_1\right)^2},\ p_3=\frac{K}{h_1r_1},\\ q_1 &= \frac{a_2\left(1-\nu_2\right)h_2K-1}{2a_2\left(1-\nu_2\right)h_2},\ q_2=\frac{K^2}{4}+\frac{k_2\mu_1}{h_2r_2}+\frac{K}{2a_2\left(1-\nu_2\right)h_2}+\frac{1}{4\left(a_2\left(1-\nu_2\right)h_2\right)^2},\ q_3=\frac{K}{h_2r_2}, \end{aligned} \tag{3.8}$$

and the positive value of B^* must satisfy the following equation

$$\begin{aligned}&\frac{e_2a_2(1-\nu_2)\left(q_1+\sqrt{q_2+q_3\sqrt{\mu_1^2+\mu_2B^*}-q_3B^*}\right)\left(B^*+\mu_1-\sqrt{\mu_1^2+\mu_2B^*}\right)}{1+a_2h_2\left(1-\nu_2\right)\left(q_1+\sqrt{q_2+q_3\sqrt{\mu_1^2+\mu_2B^*}-q_3B^*}\right)}\\&+\frac{e_1a_1(1-\nu_1)\left(p_1+\sqrt{p_2-p_3\sqrt{\mu_1^2+\mu_2B^*}}\right)\left(-\mu_1+\sqrt{\mu_1^2+\mu_2B^*}\right)}{1+a_1h_1\left(1-\nu_1\right)\left(p_1+\sqrt{p_2-p_3\sqrt{\mu_1^2+\mu_2B^*}}\right)}\\&-d_1\left(-\mu_1+\sqrt{\mu_1^2+\mu_2B^*}\right)-d_2\left(B^*+\mu_1-\sqrt{\mu_1^2+\mu_2B^*}\right)=0.\end{aligned} \tag{3.9}$$

3.2. Local Stability of Equilibrium Points

In this section, we derive the local stability of all equilibrium points as mentioned above using the Routh-Hurwitz criterion [30].

Theorem 3.1. *The axial equilibrium points* $E_0(0,0,0)$, $E_1(K,0,0)$, *and* $E_2(0,K,0)$ *of system* (2.18) *are always unstable.*

Proof. First, the stability of the equilibrium point E_0 of model (2.18) can be obtained by computing the Jacobian matrix at point E_0 as follows:

$$J(E_0)=\begin{bmatrix} r_1 & 0 & 0\\ 0 & r_2 & 0\\ 0 & 0 & -\frac{2\,d_2\mu_1+\mu_2(d_1-d_2)}{2\mu_1}\end{bmatrix}. \tag{3.10}$$

Now we consider the characteristic equation: $\det\|J(E_0)-\lambda I\|=0$, where λ and I are an eigenvalue and the identity matrix 3×3, respectively. Then, we have

$$\left(\lambda-r_1\right)\left(\lambda-r_2\right)\left(\lambda+\frac{2\,d_2\mu_1+\mu_2\left(d_1-d_2\right)}{2\mu_1}\right)=0. \tag{3.11}$$

From (3.11), it is obvious that at least one of the eigenvalues of the system is positive, i.e., $\lambda=r_1>0$ and $\lambda=r_2>0$. Thus, E_0 is always unstable.

Secondly, we obtain the Jacobian matrix of model (2.18) at the equilibrium point E_1 as follows:

$$J(E_1)=\begin{bmatrix} -r_1 & 0 & \frac{a_1(\nu_1-1)K\mu_2}{2\mu_1(a_1h_1K\nu_1-a_1h_1K-1)}\\ 0 & r_2 & 0\\ 0 & 0 & j_{3,3}^{E_1}\end{bmatrix}, \tag{3.12}$$

where

$$\begin{aligned}j_{3,3}^{E_1}=&\frac{\left(1-\nu_1\right)\left(\left(\left(d_1-d_2\right)h_1-e_1\right)\mu_2+2\,d_2h_1\mu_1\right)Ka_1+\mu_2\left(d_1-d_2\right)}{2\mu_1\left(h_1K\left(\nu_1-1\right)a_1-1\right)}\\&+\frac{d_2}{\left(h_1K\left(\nu_1-1\right)a_1-1\right)}.\end{aligned} \tag{3.13}$$

Next, the characteristic equation using $J(E_1)$ is

$$\det \|J(E_1) - \lambda I\| = (\lambda + r_1)(\lambda - r_2)\left(\lambda - j_{3,3}^{E_1}\right) = 0. \tag{3.14}$$

So, the equilibrium point E_1 is always unstable because $\lambda = r_2 > 0$.

Lastly, the Jacobian matrix at the equilibrium point E_2 can be expressed as

$$J(E_2) = \begin{bmatrix} r_1 & 0 & 0 \\ 0 & -r_2 & \frac{K(\nu_2-1)a_2(2\mu_1-\mu_2)}{2(a_2h_2K\nu_2-a_2h_2K-1)\mu_1} \\ 0 & 0 & j_{3,3}^{E_2} \end{bmatrix}, \tag{3.15}$$

where

$$j_{3,3}^{E_2} = \frac{a_2(1-\nu_2)K\left(\left(\left(d_1-d_2\right)h_2+e_2\right)\mu_2+2\mu_1\left(d_2h_2-e_2\right)\right)}{2\left(a_2Kh_2\left(\nu_2-1\right)-1\right)\mu_1} + \frac{\mu_2\left(d_1-d_2\right)+2d_2\mu_1}{2\left(a_2Kh_2\left(\nu_2-1\right)-1\right)\mu_1}. \tag{3.16}$$

The characteristic equation using $J(E_2)$ can be obtained by

$$\det \|J(E_2) - \lambda I\| = (\lambda - r_1)(\lambda + r_2)\left(\lambda - j_{3,3}^{E_2}\right) = 0. \tag{3.17}$$

Since $\lambda = r_1 > 0$, we then obtain that the equilibrium point E_2 is always unstable. ■

Theorem 3.2. *If $j_{3,3}^{E_3} < 0$, where $j_{3,3}^{E_3}$ is the element in the third row and third column of the Jacobian matrix of system (2.18) evaluated at the BPH-free equilibrium point $E_3(K, K, 0)$, then the equilibrium point E_3 is locally asymptotically stable.*

Proof. The Jacobian matrix of system (2.18) at E_3 is expressed as

$$J(E_3) = \begin{bmatrix} -r_1 & 0 & -\frac{a_1(\nu_1-1)K\mu_2}{2\mu_1(a_1Kh_1(\nu_1-1))-1} \\ 0 & -r_2 & \frac{(\mu_1-\mu_2/2)(\nu_2-1)Ka_2}{(1+a_2Kh_2(1-\nu_2))\mu_1} \\ 0 & 0 & j_{3,3}^{E_3} \end{bmatrix}. \tag{3.18}$$

Consequently, the characteristic equation of $J(E_3)$ is provided by

$$(\lambda + r_1)(\lambda + r_2)\left(\lambda - j_{3,3}^{E_3}\right) = 0, \tag{3.19}$$

where

$$j_{3,3}^{E_3} = \frac{1}{s_1}\left[a_2K(1-\nu_2)\left(a_1K(\nu_1-1)s_3+s_4\right)+s_2\right], \tag{3.20}$$

where

$$\begin{aligned} s_1 &= 2\mu_1\left(a_1Kh_1\left(\nu_1-1\right)-1\right)\left(a_2Kh_2\left(\nu_2-1\right)-1\right) \neq 0, \\ s_2 &= \left(K\left(\nu_1-1\right)\left(d_1h_1-d_2h_1-e_1\right)a_1-d_1+d_2\right)\mu_2+2d_2\mu_1\left(a_1Kh_1\left(\nu_1-1\right)-1\right), \\ s_3 &= \left(\left(\left(d_1-d_2\right)h_2+e_2\right)\mu_2+2\mu_1\left(d_2h_2-e_2\right)\right)h_1-\mu_2e_1h_2, \\ s_4 &= \left(\left(-d_1+d_2\right)h_2-e_2\right)\mu_2-2\mu_1\left(d_2h_2-e_2\right). \end{aligned} \tag{3.21}$$

From (3.19), we find that $\lambda = -r_1 < 0$, $\lambda = -r_2 < 0$ and $\lambda = j_{3,3}(E_3)$. If it is required that $j_{3,3}(E_3) < 0$, then system (2.18) is locally stable around E_3. ■

Theorem 3.3. *The equilibrium point* $E_4(0, \hat{R}_2, \hat{B})$ *is locally asymptotically stable if*

$$N_1 < 0, \quad N_2 > 0 \quad \text{and} \quad N_3 > 0, \tag{3.22}$$

where N_1, N_2 *and* N_3 *are the coefficients of* λ *in the characteristic equation of the variational matrix of system* (2.18) *evaluated at* E_4 *which can be arranged in the form*

$$(\lambda - N_1)\left(\lambda^2 + N_2\lambda + N_3\right) = 0. \tag{3.23}$$

Proof. The Jacobian matrix of model (2.18) at E_4 can be expressed as

$$J(E_4) = \begin{bmatrix} j_{1,1}^{E_4} & 0 & 0 \\ 0 & j_{2,2}^{E_4} & j_{2,3}^{E_4} \\ a_1 e_1 \left(\mu_1 - \sqrt{\hat{B}\,\mu_2 + {\mu_1}^2}\right)(\nu_1 - 1) & j_{3,2}^{E_4} & j_{3,3}^{E_4} \end{bmatrix}, \tag{3.24}$$

where

$$j_{1,1}^{E_4} = r_1 + a_1(1 - \nu_1)\left(\mu_1 - \sqrt{\hat{B}\mu_2 + \mu_1^2}\right),$$

$$\begin{aligned} j_{2,2}^{E_4} = \Big[& a_2 k_2 (1 - \nu_2)\sqrt{\hat{B}\mu_2 + \mu_1^2} - (\nu_2 - 1)^2 \hat{R}_2^2 \left(2\hat{R}_2 - k_2\right) r_2 h_2^2 a_2^2 \\ &+ a_2(\nu_2 - 1)\left(\left(-2\,\hat{R}_2\, h_2 r_2 + \hat{B} + \mu_1\right) k_2 + 4\,\hat{R}_2^2 h_2 r_2\right) \\ &- \left(2\,\hat{R}_2 - k_2\right) r_2 \Big] \times \left(k_2\left(-1 + \hat{R}_2\, h_2\,(\nu_2 - 1)\, a_2\right)^2\right)^{-1}, \end{aligned}$$

$$j_{2,3}^{E_4} = \frac{a_2(1 - \nu_2)\,\hat{R}_2\left(2\sqrt{\hat{B}\,\mu_2 + \mu_1^2} - \mu_2\right)}{2\left(\hat{R}_2\, a_2 h_2 \nu_2 - \hat{R}_2\, a_2 h_2 - 1\right)\sqrt{\hat{B}\,\mu_2 + \mu_1^2}},$$

$$j_{3,2}^{E_4} = -\frac{e_2 a_2(\nu_2 - 1)\left(\hat{B} + \mu_1 - \sqrt{\hat{B}\,\mu_2 + \mu_1^2}\right)}{\left(-1 + \hat{R}_2\, h_2\,(\nu_2 - 1)\, a_2\right)^2},$$

$$\begin{aligned} j_{3,3}^{E_4} = -\Big[& \left(2\hat{R}_2\,(\nu_2 - 1)(d_2 h_2 - e_2)\, a_2 - 2\, d_2\right)\sqrt{\hat{B}\,\mu_2 + \mu_1^2} \\ &+ \mu_2\left(\hat{R}_2\,(v_2 - 1)\left((d_1 - d_2)\, h_2 + e_2\right) a_2 - d_1 + d_2\right)\Big] \\ &\times \left(\sqrt{\hat{B}\,\mu_2 + \mu_1^2}\left(-2 + 2\,\hat{R}_2\, h_2\,(v_2 - 1)\, a_2\right)\right)^{-1}. \end{aligned}$$

Then, the characteristic equation of $J(E_4)$ is in the following form

$$(\lambda - N_1)\left(\lambda^2 + N_2\lambda + N_3\right) = 0,$$

where

$$N_1 = j_{1,1}^{E_4}, \quad N_2 = -j_{2,2}^{E_4} - j_{3,3}^{E_4} \text{ and } N_3 = j_{2,2}^{E_4} j_{3,3}^{E_4} - j_{2,3}^{E_4} j_{3,2}^{E_4}. \tag{3.25}$$

If N_1, N_2, N_3 in (3.25) are such that $N_1 < 0$, $N_2 > 0$ and $N_3 > 0$, then the locally asymptotic stability of the equilibrium point E_4 is established by the Routh-Hurwitz criterion. ■

Theorem 3.4. *The equilibrium point $E_5(\tilde{R}_1, 0, \tilde{B})$ is locally asymptotically stable if*

$$S_1 < 0, \quad S_2 > 0 \quad \text{and} \quad S_3 > 0, \tag{3.26}$$

where S_1, S_2 and S_3 are the coefficients of λ in the characteristic equation of the variational matrix of system (2.18) evaluated at E_5 which can be written in the form

$$(\lambda - S_1)\left(\lambda^2 + S_2\lambda + S_3\right) = 0. \tag{3.27}$$

Proof. The Jacobian matrix of model (2.18) evaluated at E_5 is as follows

$$J(E_5) = \begin{bmatrix} j_{1,1}^{E_5} & 0 & j_{1,3}^{E_5} \\ 0 & j_{2,2}^{E_5} & 0 \\ j_{3,1}^{E_5} & e_2 a_2 (1 - v_2)\left(\tilde{B} + \mu_1 - \sqrt{\tilde{B}\,\mu_2 + \mu_1^2}\right) & j_{3,3}^{E_5} \end{bmatrix}, \tag{3.28}$$

where

$$\begin{aligned} j_{1,1}^{E_5} =& \Big\{a_1 K (\nu_1 - 1)\sqrt{\tilde{B}\,\mu_2 + \mu_1^2} - h_1^2 r_1 \tilde{R}_1^2 \left(2\tilde{R}_1 - K\right)(\nu_1 - 1)^2 a_1^2 \\ &+ \left(4\tilde{R}_1^2 h_1 r_1 - 2\tilde{R}_1 h_1 K r_1 - k_1 \mu_1\right)(\nu_1 - 1)\, a_1 - r_1 \left(2\tilde{R}_1 - K\right)\Big\} \\ &\times \left(\left(a_1 \tilde{R}_1 h_1 (\nu_1 - 1) - 1\right)^2 K\right)^{-1}, \end{aligned}$$

$$\begin{aligned} j_{2,2}^{E_5} =& (1 - \nu_2)\, a_2 \sqrt{\tilde{B}\mu_2 + \mu_1^2} + (\nu_2 - 1)\left(\tilde{B} + \mu_1\right) a_2 + r_2, \\ j_{1,3}^{E_5} =& \frac{a_1 (\nu_1 - 1)\,\tilde{R}_1\,\mu_2}{2\sqrt{\tilde{B}\,\mu_2 + {\mu_1}^2}\left(1 - a_1 \tilde{R}_1\, h_1 (\nu_1 - 1)\right)}, \\ j_{3,1}^{E_5} =& \frac{e_1 a_1 \left(\mu_1 - \sqrt{\tilde{B}\,\mu_2 + {\mu_1}^2}\right)(\nu_1 - 1)}{\left(a_1 \tilde{R}_1 h_1 (\nu_1 - 1) - 1\right)^2}, \\ j_{3,3}^{E_5} =& \frac{\mu_2 \left((\nu_1 - 1)\left((d_1 - d_2)\, h_1 - e_1\right)\tilde{R}_1\, a_1 - d_1 + d_2\right)}{2\sqrt{\tilde{B}\,\mu_2 + {\mu_1}^2}\left(1 - a_1 \tilde{R}_1\, h_1 (\nu_1 - 1)\right)} - d_2. \end{aligned}$$

The characteristic equation of the above matrix can be written in the following form

$$(\lambda - S_1)\left(\lambda^2 + S_2\lambda + S_3\right) = 0,$$

where

$$S_1 = j_{2,2}^{E_5}, \quad S_2 = -j_{1,1}^{E_5} - j_{3,3}^{E_5}, \quad S_3 = j_{1,1}^{E_5} j_{3,3}^{E_5} - j_{1,3}^{E_5} J_{3,1}^{E_5}. \tag{3.29}$$

If S_1, S_2, S_3 in (3.29) are such that $S_1 < 0$, $S_2 > 0$ and $S_3 > 0$, then, by the Routh-Hurwitz criterion, the equilibrium point E_5 is locally asymptotically stable. Otherwise, the system is unstable at E_5. ∎

Theorem 3.5. *The equilibrium point $E^*(R_1^*, R_2^*, B^*)$ is locally asymptotically stable if the following conditions hold:*

$$P_1 > 0,\ P_2 > 0,\ P_3 > 0,\ \text{and } P_1P_2 > P_3, \tag{3.30}$$

where P_1, P_2, P_3 are the coefficients of λ in the characteristic equation of the variational matrix of system (2.18) evaluated at E^* which can be written in the form

$$\lambda^3 + P_1\lambda^2 + P_2\lambda + P_3 = 0. \tag{3.31}$$

Proof. The Jacobian matrix of system (2.18) at E^* is

$$J(E^*) = \begin{bmatrix} j_{1,1}^{E^*} & 0 & j_{1,3}^{E^*} \\ 0 & j_{2,2}^{E^*} & j_{2,3}^{E^*} \\ j_{3,1}^{E^*} & j_{3,2}^{E^*} & j_{3,3}^{E^*} \end{bmatrix}, \tag{3.32}$$

where

$$\begin{aligned}
j_{1,1}^{E^*} &= r_1\left(1-\frac{R_1^*}{K}\right) - \frac{r_1R_1^*}{K} - \frac{a_1(1-\nu_1)\left(-\mu_1+\sqrt{\mu_1^2+\mu_2B^*}\right)}{1+a_1h_1(1-\nu_1)R_1^*} \\
&\quad + \frac{a_1^2(1-\nu_1)^2R_1^*h_1\left(-\mu_1+\sqrt{\mu_1^2+\mu_2B^*}\right)}{(1+a_1h_1(1-\nu_1)R_1^*)^2}, \\
j_{1,3}^{E^*} &= -\frac{a_1(1-\nu_1)R_1^*\mu_2}{2(1+a_1h_1(1-\nu_1)R_1^*)\sqrt{\mu_1^2+\mu_2B^*}}, \\
j_{2,2}^{E^*} &= r_2\left(1-\frac{R_2^*}{K}\right) - \frac{r_2R_2^*}{K} - \frac{a_2(1-\nu_2)\left(B^*+\mu_1-\sqrt{\mu_1^2+\mu_2B^*}\right)}{1+a_2h_2(1-\nu_2)R_2^*} \\
&\quad + \frac{a_2^2(1-\nu_2)^2R_2^*h_2\left(B^*+\mu_1-\sqrt{\mu_1^2+\mu_2B^*}\right)}{(1+a_2h_2(1-\nu_2)R_2^*)^2}, \\
j_{2,3}^{E^*} &= -\frac{a_2(1-\nu_2)R_2^*}{1+a_2(1-\nu_2)h_2R_2^*}\left(1-\frac{\mu_2}{2\sqrt{\mu_1^2+\mu_2B^*}}\right),
\end{aligned}$$

$$\begin{aligned}
j_{3,1}^{E^*} &= \frac{e_1a_1(1-\nu_1)\left(-\mu_1+\sqrt{\mu_1^2+\mu_2B^*}\right)}{1+a_1(1-\nu_1)h_1R_1^*} + \frac{e_1(a_1(1-\nu_1))^2\left(-\mu_1+\sqrt{\mu_1^2+\mu_2B^*}\right)R_1^*h_1}{(1+a_1(1-\nu_1)h_1R_1^*)^2}, \\
j_{3,2}^{E^*} &= \frac{e_2a_2(1-\nu_2)B^*}{a_2(1-\nu_2)h_2R_2^*+1} - \frac{e_2a_2^2(1-\nu_2)^2R_2^*B^*h_2}{(a_2(1-\nu_2)R_2^*+1)^2} - \frac{e_2a_2(1-\nu_2)\left(-\mu_1+\sqrt{B^*\mu_2+{\mu_1}^2}\right)}{a_2(1-\nu_2)h_2R_2^*+1} \\
&\quad + \frac{e_2a_2^2(1-\nu_2)^2R_2^*\left(-\mu_1+\sqrt{B^*\mu_2+{\mu_1}^2}\right)h_2}{(a_2(1-\nu_2)h_2R_2^*+1)^2}, \\
j_{3,3}^{E^*} &= \frac{e_1a_1(1-\nu_1)R_1^*\mu_2}{2(a_1(1-\nu_1)h_1R_1^*+1)\sqrt{B^*\mu_2+\mu_1^2}} - \frac{d_1\mu_2}{2\sqrt{B^*\mu_2+\mu_1^2}} + \frac{e_2a_2(1-\nu_2)R_2^*}{a_2(1-\nu_2)h_2R_2^*+1} \\
&\quad - \frac{e_2a_2(1-\nu_2)R_2^*\mu_2}{2(a_2(1-\nu_2)h_2R_2^*+1)\sqrt{B^*\mu_2+\mu_1^2}} + \frac{d_2\mu_2}{2\sqrt{B^*\mu_2+\mu_1^2}} - d_2.
\end{aligned}$$

Then, the characteristic equation of the matrix $J(E^*)$ can be obtained in the following form

$$\lambda^3 + P_1\lambda^2 + P_2\lambda + P_3 = 0,$$

where

$$\begin{aligned} P_1 &= -j_{3,3}^{E^*} - j_{2,2}^{E^*} - j_{1,1}^{E^*}, \\ P_2 &= -j_{1,3}^{E^*} j_{3,1}^{E^*} - j_{2,3}^{E^*} j_{3,2}^{E^*} + j_{1,1}^{E^*} j_{3,3}^{E^*} + j_{1,1}^{E^*} j_{2,2}^{E^*} + j_{2,2}^{E^*} j_{3,3}^{E^*}, \\ P_3 &= -j_{1,1}^{E^*} j_{2,2}^{E^*} j_{3,3}^{E^*} + j_{1,1}^{E^*} j_{2,3}^{E^*} j_{3,2}^{E^*} + j_{1,3}^{E^*} j_{2,2}^{E^*} j_{3,1}^{E^*}. \end{aligned} \tag{3.33}$$

Using the Routh-Hurwitz criterion for the necessary and sufficient conditions for the locally asymptotic stability of system (2.18) at E^*, if

$$P_i > 0, \ (i = 1, 2, 3), \qquad \text{and} \qquad P_1 P_2 > P_3. \tag{3.34}$$

hold, then the equilibrium point E^* is locally asymptotically stable. Hence, Theorem 3.5 is proved. ∎

3.3. Hopf Bifurcation

In this section, we study the Hopf bifurcation [31] of the aggregated model (2.18) at the equilibrium point $E_4(0, \hat{R}_2, \hat{B})$ when the the maximum carrying capacity K is taken as a bifurcation parameter. Expanding the characteristic equation (3.23), we obtain its alternative form as

$$\lambda^3 + U_1\lambda^2 + U_2\lambda + U_3 = 0, \tag{3.35}$$

where $U_1 = U_1(K) = N_2 - N_1$, $U_2 = U_2(K) = N_3 - N_1N_2$ and $U_3 = U_3(K) = -N_1N_3$.

Now, we define

$$f(K) = U_3(K) - U_1(K)U_2(K). \tag{3.36}$$

Theorem 3.6. *If there exists $K = K^*$ satisfying the following conditions:*

$$U_2(K^*) > 0, \ U_3(K^*) > 0, \ f(K^*) = 0 \text{ and } f'(K^*) \neq 0, \tag{3.37}$$

then system (2.18) gives a Hopf bifurcation at $K = K^*$ or there is a limit cycle around the equilibrium point E_4.

Proof. It is possible to find a positive value $K = K^*$ such that $U_2(K^*) > 0$, $U_3(K^*) > 0$ and $f(K^*) = 0$. Next, it must verify that the Hopf bifurcation condition $f'(K^*) \neq 0$ holds. By substituting $\lambda = \gamma + i\beta$ into (3.35), we obtain

$$\gamma^3 - 3\gamma\beta^2 + \left(3\gamma^2\beta - \beta^3\right) i + U_3\left(\gamma^2 + 2\gamma\beta i - \beta^2\right) + U_2\left(\gamma + i\beta\right) + U_3 = 0. \tag{3.38}$$

Separating real and imaginary parts of (3.38), we get the real part as

$$\gamma^3 - 3\gamma\beta^2 + U_1\left(\gamma^2 - \beta^2\right) + U_2\gamma + U_3 = 0, \tag{3.39}$$

and the imaginary part as

$$3\gamma^2 - \beta^2 + 2\,U_1\gamma + U_2 = 0. \tag{3.40}$$

From (3.40), we get $\beta^2 = 3\gamma^2 + 2\,U_1\gamma + U_2$. Replacing the value of β^2 into (3.39), we then get

$$8\gamma^3 + 8\,U_1\gamma^2 + 2(U_1^2 + U_2)\gamma + U_1U_2 - U_3 = 0. \tag{3.41}$$

Differentiating Eq. (3.41) with respect to K, substituting $K = K^*$ and $\gamma(K^*) = 0$ into the resulting equation, we have

$$\begin{aligned}\left[\frac{d\mathrm{Re}(\lambda)}{dK}\right]\bigg|_{K=K^*} &= \left(\frac{d\gamma}{dK}\right)\bigg|_{K=K^*} \\ &= \frac{U_3'(K^*) - (U_1(K^*)U_2'(K^*) + U_1'(K^*)U_2(K^*))}{2(U_1^2(K^*) + U_2(K^*))} \neq 0.\end{aligned} \tag{3.42}$$

The above result can be obtained using the assumption $f'(K^*) \neq 0$. Hence, the transversality condition of the Hopf bifurcation at point $K = K^*$ is derived and consequently the theorem is proved. ■

4. Numerical Simulations and Discussions

In this section, we use numerical simulations of model (2.18) to illustrate its stability, and the effects of the carrying capacity, monsoon factors and habitat complexity factors. We also give a discussion of the numerical results.

4.1. Stability of the Model

In this section, we study the local asymptotic stability of the equilibrium points of model (2.18) for a range of parameter values. Some parameter values are taken from research findings for actual BPH infestations reported in [27, 32] such as monsoon rate, attack rate, conversion rate, intrinsic growth rate and death rate of BPH. We begin by showing some numerical results for the equilibrium point $E_3(K, K, 0)$ of model (2.18) by using the parameter set in Eq. (4.1) and the initial conditions $R_1(0) = 5$, $R_2(0) = 23$ and $B(0) = 2$. Figure 3 shows that system (2.18) has a local asymptotically stable equilibrium point $E_3(10, 10, 0)$ in which both the rice in field 1 and field 2 converge to the maximum capacity of rice $K = 10$ and the total population of BPH eventually disappears.

$$\begin{aligned}&r_1 = 0.1,\ d_1 = 0.18,\ e_1 = 0.067,\ a_1 = 0.15,\ h_1 = 0.2,\ \nu_1 = 0.15,\\ &r_2 = 0.08,\ d_2 = 0.15,\ e_2 = 0.068,\ a_2 = 0.1, h_2 = 0.1,\ \nu_2 = 0.2,\\ &K = 10,\ m_0 = 0.3,\ m_1 = 0.1,\ \bar{m} = 0.2.\end{aligned} \tag{4.1}$$

With the parameter set in Eq. (4.1), we have $j_{3,3}^{E_3} = -0.1045 < 0$ and consequently the numerical results agree with Theorem 3.2 for the equilibrium point E_3.

Next, we investigate the local asymptotic stability of the equilibrium point $E_4(0, \hat{R}_2, \hat{B})$ of system (2.18). We use the parameter set in Eq. (4.2), initial conditions $R_1(0) = 10$, $R_2(0) = 20$ and $B(0) = 10$, carrying capacity $K = 150$ and with the growth rate of BPH for field 1 (r_1) much less than field 2 (r_2). The results in Figure 4 show that the equilibrium point $E_4(0, 55.78, 12.10)$ in which the rice in field 1 eventually decreases to zero is locally asymptotically stable.

$$\begin{aligned}&r_1 = 0.01,\ d_1 = 0.18,\ e_1 = 0.067,\ a_1 = 0.15,\ h_1 = 0.2,\ \nu_1 = 0.15,\\ &r_2 = 0.8,\ d_2 = 0.15,\ e_2 = 0.068,\ a_2 = 0.1, h_2 = 0.1,\ \nu_2 = 0.2,\\ &K = 150,\ m_0 = 0.3,\ m_1 = 0.1,\ \bar{m} = 0.2.\end{aligned} \tag{4.2}$$

Since the assumptions of Theorem 3.3 are satisfied, i.e., $N_1 = -0.3748 < 0$, $N_2 = 0.1260 > 0$ and $N_3 = 0.05736 > 0$, then the numerical results agree with the theorem for the equilibrium point E_4 as shown in Figure 4.

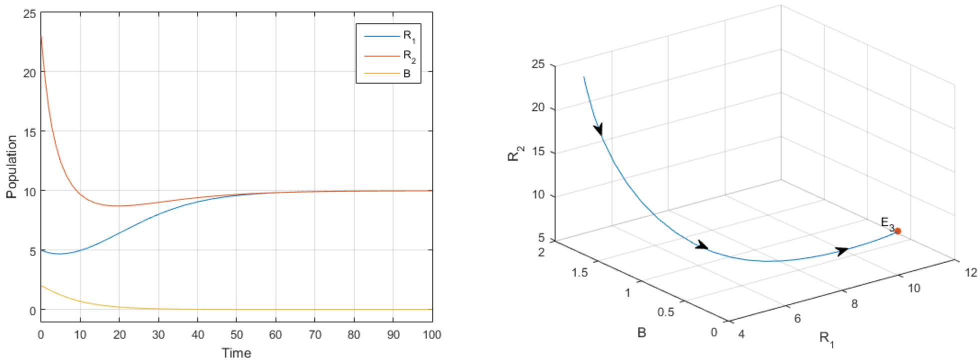

(A) (B)

FIGURE 3. Numerical simulations of population densities of model (2.18) using the parameter set (4.1) in case of the locally asymptotically stable equilibrium point E_3: (a) Time series solutions of R_1, R_2, and B, (b) Phase portrait of R_1, R_2, and B.

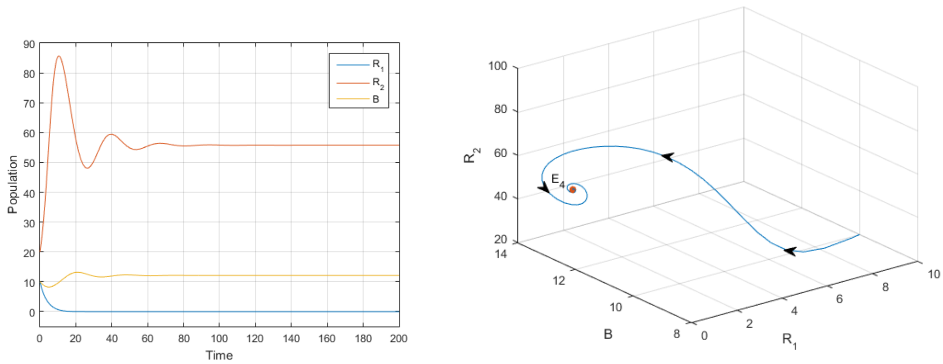

(A) (B)

FIGURE 4. Numerical simulations of population densities of model (2.18) using the parameter set (4.2) in case of the locally asymptotically stable equilibrium point E_4: (a) Time series solutions of R_1, R_2, and B, (b) Phase portrait of R_1, R_2, and B.

Using the parameter set in Eq. (4.1), except changing the parameter K from $K = 10$ to $K = 300$ and the handling time of BPH in field 1 (h_1) from 0.2 to 0.02, we use the parameter set in Eq. (4.3) to study the local asymptotic stability of the equilibrium point $E_5(\tilde{R}_1, 0, \tilde{B})$ of system (2.18). Applying the initial conditions $R_1(0) = 80$, $R_2(0) = 1$, and $B(0) = 10$ and the parameter values in (4.3) for system (2.18), we find that the equilibrium point $E_5(62.26, 0, 2.05)$ is locally asymptotic stable as displayed in Figure 5. It can be observed that when the predator's capture time h_2 is longer than h_1 and the monsoon takes more BPHs to field 2, i.e., $m_0 + m_1 > \bar{m}$, the extinction behavior of rice in field 2 due to the BPH's attack eventually appears. However, the density of rice in field 1 oscillates in the early period and finally grows constantly.

$$\begin{aligned} &r_1 = 0.1,\ d_1 = 0.18,\ e_1 = 0.067,\ a_1 = 0.2,\ h_1 = 0.02,\ \nu_1 = 0.15, \\ &r_2 = 0.08,\ d_2 = 0.15,\ e_2 = 0.068,\ a_2 = 0.1, h_2 = 0.1,\ \nu_2 = 0.2, \\ &K = 300,\ m_0 = 0.3,\ m_1 = 0.1,\ \bar{m} = 0.2. \end{aligned} \tag{4.3}$$

The above numerical results agree with the asymptotic convergence to E_5 of system 2.18 stated in Theorem 3.4 because $S_1 = -0.0271 < 0$, $S_2 = 0.0266 > 0$ and $S_3 = 0.00045 > 0$.

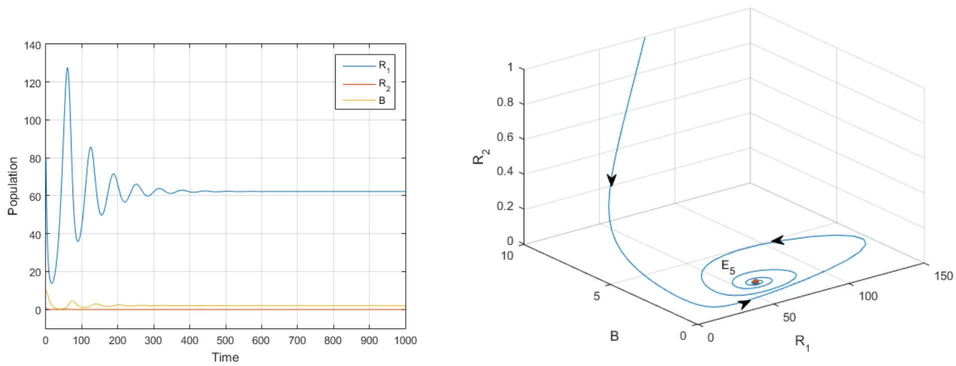

(A) (B)

FIGURE 5. Numerical simulations of population densities of model (2.18) using the parameter set (4.3) in case of the locally asymptotically stable equilibrium point E_5: (a) Time series solutions of R_1, R_2, and B, (b) Phase portrait of R_1, R_2, and B.

In Figure 6, the parameter set (4.1) is used for model (2.18) except changing from $K = 10$ to $K = 100$. In consequence, the solution behavior of the system changes from converging to E_3 to converging to $E^*(R_1^*, R_2^*, B^*)$. For the parameter set (4.4) and the initial conditions $R_1(0) = 40$, $R_2(0) = 20$ and $B(0) = 10$, system (2.18) has the co-existence equilibrium point $E^*(78.69, 28.18, 1.38)$ which is locally asymptotically stable as shown in Figure 6. In addition, the solutions $R_1(t)$, $R_2(t)$ and $B(t)$ oscillate in the beginning but eventually stay constant and converge to $E^*(78.69, 28.18, 1.38)$.

$$\begin{aligned} &r_1 = 0.1,\ d_1 = 0.18,\ e_1 = 0.067,\ a_1 = 0.15,\ h_1 = 0.2,\ \nu_1 = 0.15, \\ &r_2 = 0.08,\ d_2 = 0.15,\ e_2 = 0.068,\ a_2 = 0.1, h_2 = 0.1,\ \nu_2 = 0.2, \\ &K = 100,\ m_0 = 0.3,\ m_1 = 0.1,\ \bar{m} = 0.2. \end{aligned} \tag{4.4}$$

By numerical computations obtained by using the parameter set (4.4), we have $P_1 = 0.0785 > 0$, $P_2 = 0.0053 > 0$, $P_3 = 0.00026 > 0$ and $P_1P_2 - P_3 = 0.00016 > 0$ corresponding to the Routh-Hurwitz criterion (3.30). Hence, the numerical results agree with Theorem 3.5.

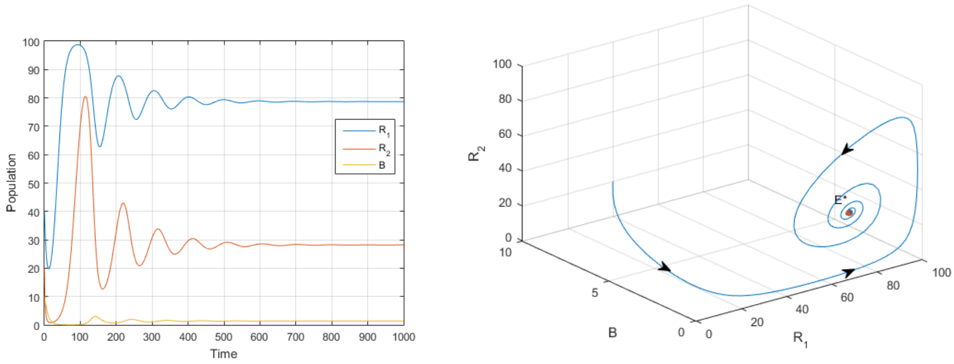

(A) (B)

FIGURE 6. Numerical simulations of population densities of model (2.18) using the parameter set (4.4) in case of the locally asymptotically stable equilibrium point E^*: (a) Time series solutions of R_1, R_2, and B, (b) Phase portrait of R_1, R_2, and B.

4.2. Impact of the Carrying Capacity

In this section, the stability of model (2.18) is investigated through the Hopf bifurcation parameter K, which is the maximum carrying capacity of rice for each field (i.e., the field area). Taking the parameter set in Eq. (4.2) and using the initial conditions $R_1(0) = 10$, $R_2(0) = 20$ and $B(0) = 10$ with the bifurcation parameter K, Theorem 3.6 will be numerically checked about the equilibrium point E_4. The critical value $K^* = 219.31$ for Hopf bifurcation is calculated utilizing the conditions in (3.37). Figure 7 shows that when $K = 201 < K^*$, the model is asymptotically stable around the equilibrium point $E_4(0, 54.59, 13.98)$. In addition, when $K = K^* = 219.31$, the system (2.18) undergoes a Hopf bifurcation at the equilibrium point $E_4(0, 54.47, 14.17)$ as shown in Figure 8. Ultimately, when $K = 250 > K^*$, the system (2.18) has a limit cycle around the equilibrium point $E_4(0, 54.18, 14.69)$ as shown in Figure 9. Precisely speaking, the model (2.18) has the Hopf bifurcation at E_4 for $K \geq K^*$. This can be numerically obtained by simulating the model with the above parameter set and the initial conditions, 30,000 time steps and $K \in [150, 400]$ and collecting the maximum and minimum population density variables. Figure 10 demonstrates the Hopf bifurcation diagrams of rice in field 2 (R_2) and the total BPH (B) with respect to K. It can be seen from the diagrams in Figure 10 that when $K < K^* = 219.31$, then the model's behavior (i.e., R_2 and B) is asymptotically stable around E_4 and when $K > K^* = 219.31$, then the behavior of R_2 and B alters from stable focus to unstable state with oscillations between maximum and minimum values. Consequently, if the field area K is increased, then the instability of the BPHrice system also increases.

Moreover, Figure 11 shows the intervals of K such that the equilibrium points E_3, E_4, E_5 and E^* are asymptotically stable for the parameter sets (4.1), (4.2), (4.3), (4.4), respectively as mentioned in section 4.1. The intervals of K for stability of the equilibrium points E_3, E_4, E_5 and E^* are shown in Figures 11(a), (b), (c) and (d), respectively.

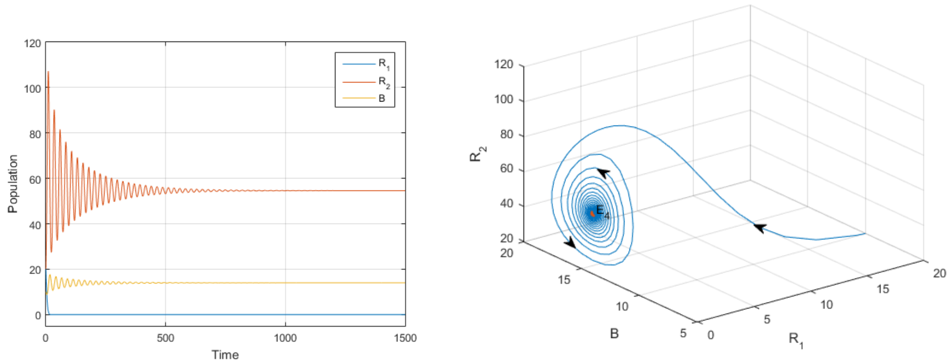

(A) (B)

FIGURE 7. Solution behavior of system (2.18) when the parameter set (4.2), the initial values $R_1(0) = 20$, $R_2(0) = 20$, $B(0) = 10$ and $K = 201 < K^* = 219.31$ are used. The solution asymptotically converges to the equilibrium point $E_4(0, 54.59, 13.98)$: (a) Time series solutions of R_1, R_2, and B, (b) Phase plot of R_1, R_2, and B.

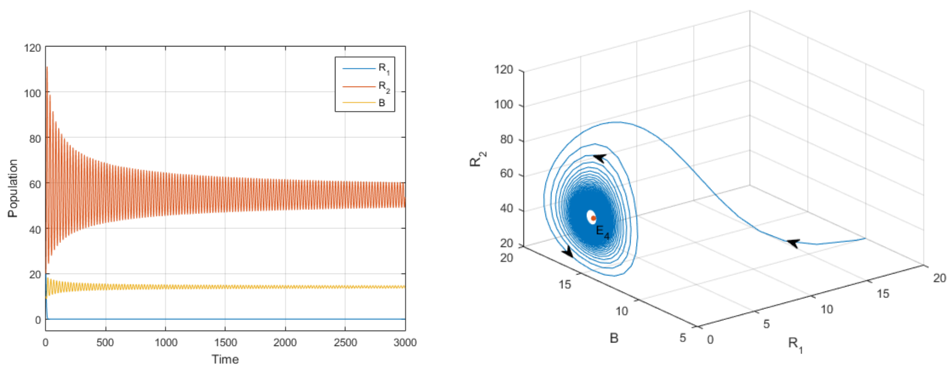

(A) 2D (B) 3D

FIGURE 8. Solution behavior of system (2.18) when the parameter set (4.2), the initial values $R_1(0) = 20$, $R_2(0) = 20$, $B(0) = 10$ and $K = K^* = 219.31$ are used. The solution oscillates around the equilibrium point $E_4(0, 54.47, 14.17)$: (a) Time series solutions of R_1, R_2, and B, (b) Phase plot of R_1, R_2, and B.

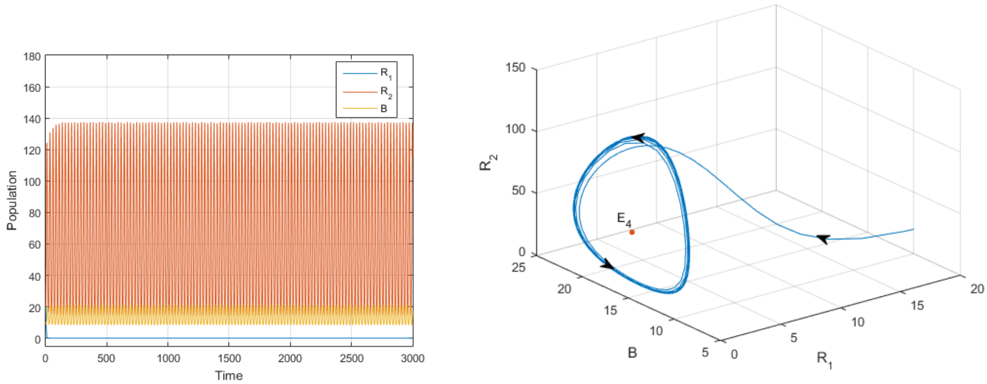

(A) 2D (B) 3D

FIGURE 9. Solution behavior of system (2.18) when the parameter set (4.2), the initial values $R_1(0) = 20$, $R_2(0) = 20$, $B(0) = 10$ and $K = 250 > K^* = 219.31$ are used. The solution oscillates around the equilibrium point $E_4(0, 54.18, 14.69$: (a) Time series solutions of R_1, R_2, and B, (b) Phase plot of R_1, R_2, and B.

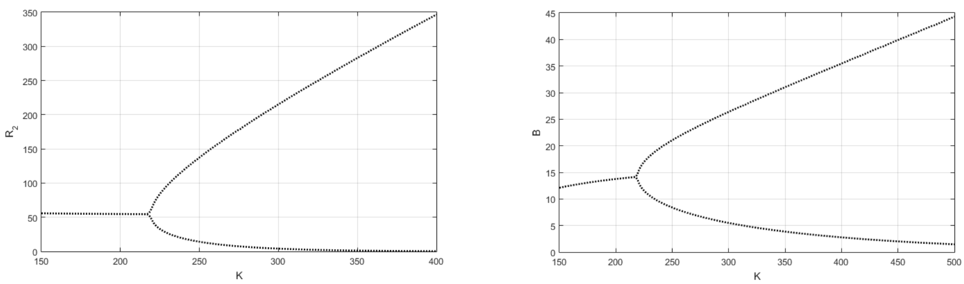

(A) (B)

FIGURE 10. Hopf bifurcation diagrams for population density of rice in field 2 and total BPH with respect to the bifurcation parameter K.

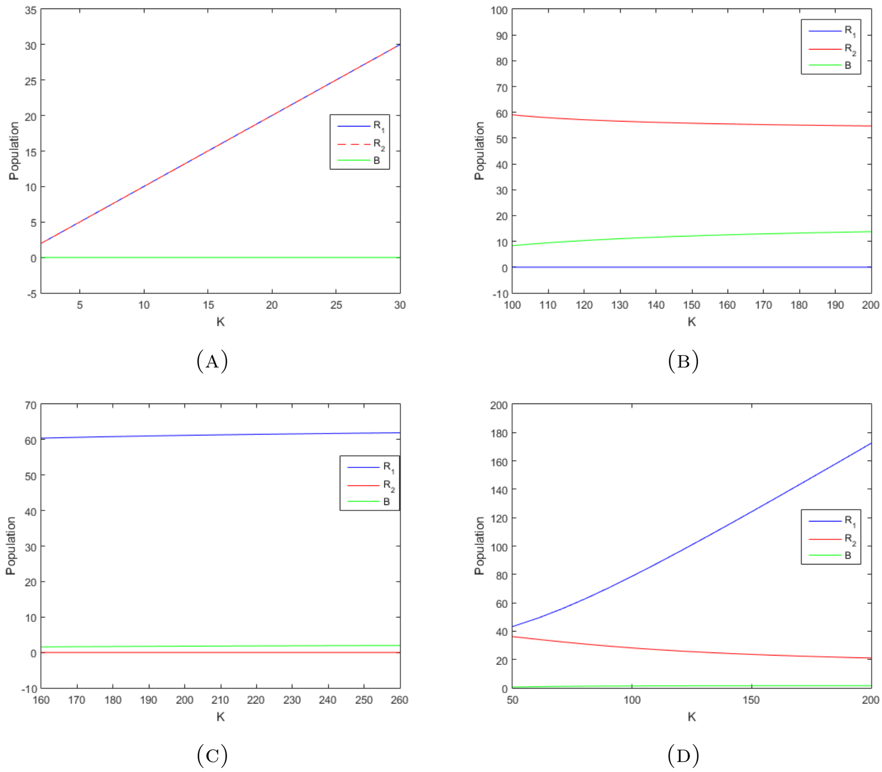

FIGURE 11. Intervals of K for which the equilibrium points are asymptotically stable: (a) E_3, (b) E_4, (c) E_5, (d) E^*.

4.3. Impact of the Monsoon Factors

In this section, the effects of the monsoon factors m_0, m_1 and $\bar{m}$ on model (2.18) are numerically examined. Using the parameter set (4.2) and varying the values of the monsoon factors, the intervals of m_0, m_1 and $\bar{m}$ in which the equilibrium point E_4 is stable are shown in Figure 12(a), (b) and (c), respectively. In Figure 12, the population density of the stable variable R_1 of E_4 decreases when the value of m_0, m_1 increases while if $\bar{m}$ becomes higher, then the density of R_1 quickly grows.

Similarly, we use the parameter set (4.3) and vary the values of the monsoon factors for model (2.18), then the intervals of m_0, m_1 and $\bar{m}$ in which the equilibrium point E_5 is stable are displayed in Figure 13(a), (b) and (c), respectively. From the current figure, when the value of m_0, m_1 increases, then the population density of the stable variable R_1 of E_5 grows linearly, on the other hand, when $\bar{m}$ increases, then the population density of R_1 is reduced.

In the same manner, the dependence of the stability of the equilibrium point E^* on the values of m_0, m_1 and $\bar{m}$ can be observed from Figure 14(a), (b) and (c), respectively. We can see from Figure 14 that the population density of the stable variable R_1 of E^* grows when the parameters m_0, m_1 increase while if $\bar{m}$ increases, then the population density of R_1 is drastically reduced.

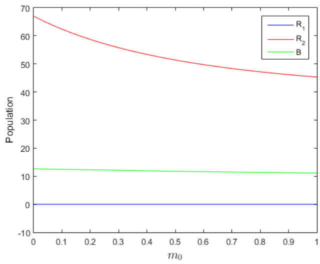

(A)

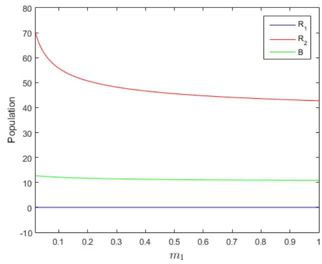

(B)

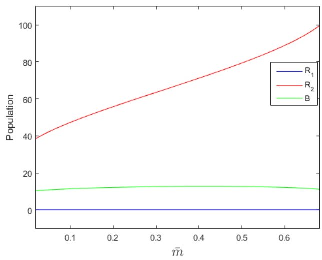

(C)

FIGURE 12. Effects of the monsoon factors on the stability of the equilibrium point E_4 of model (2.18): (a) m_0, (b) m_1, (c) $\bar{m}$.

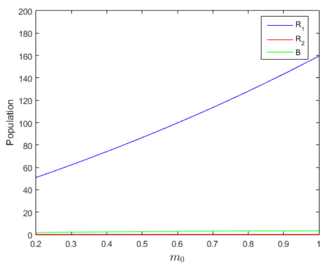

(A)

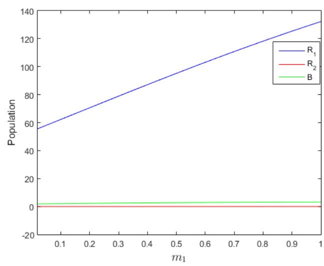

(B)

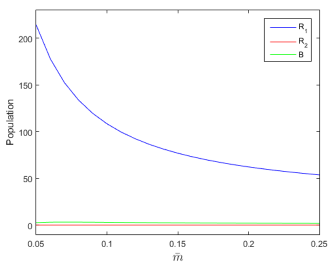

(C)

FIGURE 13. Effects of the monsoon factors on the stability of the equilibrium point E_5 of model (2.18): (a) m_0, (b) m_1, (c) $\bar{m}$.

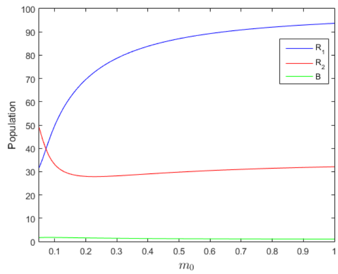

(A) m_0

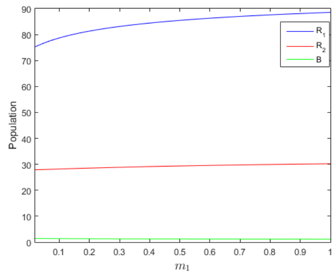

(B) m_1

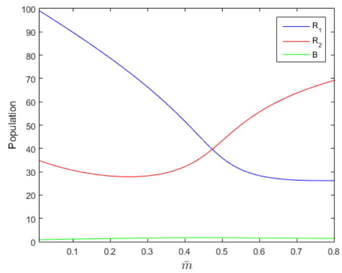

(C) $\bar{m}$

FIGURE 14. Effects of the monsoon factors on the stability of the equilibrium point E^* of model (2.18): (a) m_0, (b) m_1, (c) $\bar{m}$.

4.4. Impact of the Habitat Complexity Factors

In this section, we study the impact of habitat complexity factors in field 1 (ν_1) and field 2 (ν_2) on model (2.18). Using the parameter set (4.2) for system (2.18), we obtain the intervals of ν_1 and ν_2, in which the equilibrium point E_4 is stable shown in Figure 15(a) and (b), respectively. It can be noticed from Figure 15(b) that ν_2 strongly affects the growth of the stable variable R_2.

In the same manner, we use the parameter set (4.3) and vary the values of the habitat complexity factors for system (2.18). We find the intervals of ν_1 and ν_2 in which the equilibrium point E_5 is stable shown in Figure 15(c) and (d), respectively. It can be observed from Figure 15(c) that small values of ν_1 strongly affects the growth of the stable variable R_1.

Finally, we use the values of the parameters in Eq. (4.4) and a range of degrees of the habitat complexity in field 1 (ν_1) and field 2 (ν_2) to study the effect on system (2.18). Figures 15(e) and (f) show the intervals of ν_1 and ν_2, respectively, in which the co-existence equilibrium point E^* is stable. From these figures, the parameters ν_1 and ν_2 clearly have a distinct effect on the growth of the stable variables R_1 and R_2 of E^*.

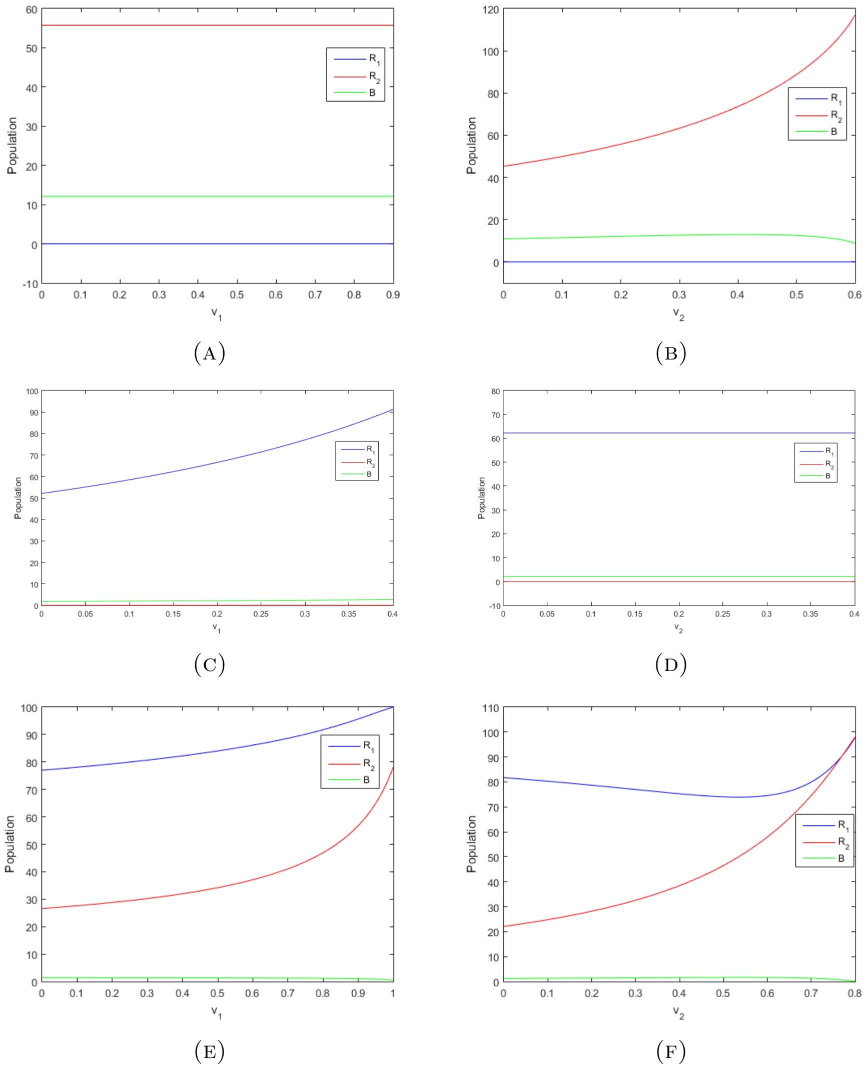

Figure 15. Stability diagrams of population densities of model (2.18) when the habitat complexity factors ν_1 and ν_2 are varied: (a)-(b) for E_4, (c)-(d) for E_5, (e)-(f) for E^*.

5. Conclusions

In this paper, we studied predator-prey models of BPH infestation of rice fields which included the effects of the monsoon and habitat complexity. We discussed two mathematical models, namely a complete model as a system of first-order differential equations with a fast time scale and an aggregated model as a system of first-order differential equations with a slow time scale. In each model, we considered two rice fields with a monsoon wind blowing from field 1 to field 2. We assumed that the growth of rice in each field could be modeled by logistic growth with different intrinsic growth rates r_1 and r_2 for the two fields but with the same carrying capacity K. For the BPH populations, we assumed that the growth rates could be modeled by a modified Holling type II function which also included the effects of habitat complexity through a parameter $\nu, 0 < \nu < 1$. We included the effects of the monsoon through factors representing an extrinsic BHP dispersal by monsoon from field 1 to field 2 and intrinsic BHP dispersals through population density between the two fields. In both models, we assumed that rice has no naturally occurring mortality but that the BPH has naturally occurring mortality. Also, in order to simplify the models, we only considered the adult BPH population and did not include egg and larval states.

For the fast time model, we included population densities for the rice and the BPH in the two fields and proved that the solutions were nonnegative and bounded. We then assumed that the effect of the monsoon in the fast time model was to obtain equilibrium BPH population densities in the two fields. It was then possible to aggregate the BPH populations in the two fields to obtain the slow time aggregated model.

In section 3, we analyzed the behavior of the slow time system. We found that the system had seven equilibrium points $E_j(R_{1,j}, R_{2,j}, B_j)$, where $R_{1,j}$ and $R_{2,j}$ are the equilibrium population densities for rice fields 1 and 2, respectively, for the jth equilibrium point, and B_j is the total BPH density on the two fields. The seven points are as follows.

(1) The trivial point is $E_0(0, 0, 0)$.
(2) The point $E_1(K, 0, 0)$ shows maximum rice in field 1, zero rice in field 2 and zero BPH.
(3) The point $E_2(0, K, 0)$ shows zero rice in field 1, maximum rice in field 2 and zero BPH.
(4) The point $E_3(K, K, 0)$ presents maximum rice in fields 1 and 2 and zero BPH.
(5) The point $E_4(0, \hat{R}_2, \hat{B})$ gives zero rice in field 1, equilibrium rice in field 2 and nonzero BPH.
(6) The point $E_5(\tilde{R}_1, 0, \tilde{B})$ presents equilibrium rice in field 1, zero rice in field 2 and nonzero BPH.
(7) The point $E^*(R_1^*, R_2^*, B^*)$ gives nonzero rice in both fields and nonzero BPH.

We then analyzed the local asymptotic stability of each equilibrium point using the eigenvalues of the Jacobians and the Routh-Hurwitz conditions. We first proved that equilibrium points E_0, E_1 and E_2 are unstable. For the other four points, we found that the stability depended on parameter values and on the effects of the monsoon and the habitat complexity. In particular, we found that under certain conditions, point E_4 can undergo a Hopf bifurcation as the maximum capacity K of the fields is increased.

Finally, we carried out numerical simulations using the ODE45 differential solver in the MATLAB package for a range of parameter values, some of which such as monsoon rate, attack rate, conversion rate, intrinsic growth rate and death rate of BPH were obtained from real data measured by [27, 32]. By varying the parameters, we were able to study and plot detailed figures for the effects of carrying capacity, monsoon and habitat complexity factors. One simple interesting result was the stability around point E_3 when K is not large, which indicates that in the case where the area used to grow rice is not large, and together with added habitat complexity, the BPH become extinct due to an inadequate amount of rice and the rice will gradually grow to fill the space that can contain it. Alternatively, if K is greater, the stability will change to other points depending on the defined parameters.

We have provided a mathematical approach for the interaction of rice and BPH with monsoon effects and habitat complexity factors that can reduce BPH predation. In fact, BPH outbreaks are influenced by many other factors, such as: distance, precipitation, temperature, humidity, fertilizer, insecticide, government policy etc. In the future, we intend to include some of these factors in the model for greater realism. In future research, it will be interesting to compare the results reported in this paper with real data collected by a research unit in order to examine how closely our results fit with real data and to estimate the values of the model parameters from real data. Ultimately, we hope that this research will provide a guide for the analysis and control of BPH outbreaks in rice fields.

Acknowledgements

The authors are grateful to anonymous referees for the valuable comments, which have significantly improved this article. The first author is supported by the PhD scholarship between King Mongkut's University of Technology North Bangkok (KMUTNB) and National Science and Technology Development Agency (NSTDA) under Contract No. GRAD.001/2565.

References

[1] H.J. Xu, C.X. Zhang, Insulin receptors and wing dimorphism in rice planthoppers, Philosophical Transactions of the Royal Society B: Biological Sciences 372 (1713) (2017) 20150489.

[2] R. Kisimoto, Bionomics, forecasting of outbreaks and injury caused by the rice brown planthopper, Seminar on the Rice Brown Planthopper, Tokyo (Japan) (Oct 5, 1976), FFTC, ASPAC.

[3] A. Otuka, M. Matsumura, S. Sanada-Morimura, H. Takeuchi, The 2008 overseas mass migration of the small brown planthopper, Laodelphax striatellus, and subsequent outbreak of rice stripe disease in western Japan, Applied Entomology and Zoology 45 (2) (2010) 259–266.

[4] J.P. Hereward, M. Matsumura, X. Cai, A.M.A. Matias, G.H. Walter, C. Xu, Y. Wang, Migration dynamics of an important rice pest: The brown planthopper (Nilaparvata lugens) across AsiaInsights from population genomics, Evolutionary Applications 13 (9) (2020) 2449–2459.

[5] D. Jana, N. Bairagi, Habitat complexity, dispersal and metapopulations: Macroscopic study of a predator–prey system, Ecological Complexity 17 (2014) 131–139.

[6] S.S. Bell, Habitat complexity of polychaete tube-caps: Influence of architecture on dynamics of a meioepibenthic assemblage, Journal of Marine Research 43 (3) (1985) 647–671.

[7] X. Li, H. Wang, A stoichiometrically derived algal growth model and its global analysis, Mathematical Biosciences & Engineering 7 (74) (2010) 825.

[8] N.E. Humphries, H. Weimerskirch, N. Queiroz, E.J. Southall, D.W. Sims, Foraging success of biological Lévy flights recorded in situ, Proceedings of the National Academy of Sciences 109 (19) (2012) 7169–7174.

[9] P.L. James, K.L. Heck Jr, The effects of habitat complexity and light intensity on ambush predation within a simulated seagrass habitat, Journal of Experimental Marine Biology and Ecology 176 (2) (1994) 187–200.

[10] B. Christensen, L. Persson, Species–specific antipredatory behaviours: Effects on prey choice in different habitats, Behavioral Ecology and Sociobiology 32 (1) (1993) 1–9.

[11] J. Manatunge, T. Asaeda, T. Priyadarshana, The influence of structural complexity on fish–zooplankton interactions: a study using artificial submerged macrophytes, Environmental Biology of Fishes 58 (4) (2000) 425–438.

[12] R. Bastiaansen, A. Doelman, M.B. Eppinga, M. Rietkerk, The effect of climate change on the resilience of ecosystems with adaptive spatial pattern formation, Ecology Letters 23 (3) (2020) 414–429.

[13] M.J. Wade, Not just numbers: Mathematical modelling and its contribution to anaerobic digestion processes, Ecology Letters 8 (8) (2020) 888.

[14] R. Bastiaansen, A. Doelman, M.B. Eppinga, M. Rietkerk, The effect of climate change on the resilience of ecosystems with adaptive spatial pattern formation, Ecology Letters 23 (3) (2020) 414–429.

[15] R. Marsland, W. Cui, J. Gldford, P. Mehta, The Community Simulator: A Python package for microbial ecology, PLOS ONE 15 (3) (2020) 1–18.

[16] S. Kumar, A. Kumar, B. Samet, H. Dutta, A study on fractional host–parasitoid population dynamical model to describe insect species, Numerical Methods for Partial Differential Equations 37 (2) (2021) 1673–1692.

[17] O. Arino, K. Boushaba, A. Boussouar, A mathematical model of the dynamics of the phytoplankton-nutrient system, Nonlinear Analysis: Real World Applications 1 (1) (2000) 69–87.

[18] B. Ghanbari, H. Günerhan, H.M. Srivastava, An application of the Atangana-Baleanu fractional derivative in mathematical biology: A three-species predator-prey model, Chaos, Solitons & Fractals 138 (2020) 109910.

[19] J. Wang, Y. Cai, S. Fu, W. Wang, The effect of the fear factor on the dynamics of a predator-prey model incorporating the prey refuge, Chaos: An Interdisciplinary Journal of Nonlinear Science 29 (8) (2019) 083109.

[20] S. Zhang , T. Zhang, S. Yuan, Dynamics of a stochastic predator-prey model with habitat complexity and prey aggregation, Ecological Complexity 45 (2021) 100889.

[21] J.C. Poggiale, Predator-prey models in heterogeneous environment: emergence of functional response, Mathematical and computer modelling 27 (4) (1998) 63–71.

[22] P. Auger, S. Charles, M. Viala, J.C. Poggiale, Aggregation and emergence in ecological modelling: integration of ecological levels, Ecological Modelling 127 (1) (2000) 11–20.

[23] R. Mchich, P. Auger, J.C. Poggiale, Effect of predator density dependent dispersal of prey on stability of a predator–prey system, Mathematical Biosciences 206 (2) (2007) 343–356.

[24] N. Bairagi, D. Jana, On the stability and Hopf bifurcation of a delay-induced predator–prey system with habitat complexity, Applied Mathematical Modelling 37 (5) (2011) 3255–3267.

[25] N.N. Doanh, N.H. Tri, A. Pierre, Effects of refuges and density dependent dispersal on interspecific competition dynamics, Ecological Complexity 10 (2012) 26–33.

[26] N.T. Hieu, T. Brochier, N.H. Tri, P. Auger, P. Brehmer, Effect of small versus large clusters of fish school on the yield of a purse-seine small pelagic fishery including a marine protected area, Acta Biotheoretica 62 (3) (2014) 339–353.

[27] A.D. Nguyen, D.N. Do, H.D. Nguyen, T.P.Nguyen, Stability analysis and Hopf bifurcation of a brown planthopper–rice model under the effect of monsoon, Ecological Modelling 468 (2022) 109942.

[28] C.S. Holling, Some characteristics of simple types of predation and parasitism1, The Canadian Entomologist 91 (7) (1959) 385–398.

[29] M.A. Efendiev, H.J. Eberl, On positivity of solutions of semi-linear convection-diffusion-reaction systems, with applications in ecology and environmental engineering, RIMS Kyoto Kokyuroko 1542 (2007) 92–101.

[30] J.D. Murray, Mathematical Biology I: An Introduction. Interdisciplinary Applied Mathematics, Springer New York, New York, 2002.

[31] Y.A. Kuznetsov, L.A. Kuznetsov, Y. Kuznetsov, Elements of Applied Bifurcation Theory, Springer New York, New York, 1998.

[32] R. Muhamad, Z.A.M. Ahmad, N.A. Adam, Life table and population parameters of Nilaparvata lugens Stal. (Homoptera: Delphacidae) on rice, Tropical Life Sciences Research 22 (1) (2011) 25–35.